Pla Moreno, B.; Bares-Moreno, P.; Jimenez, IA.; Guardiola, C. (2022). Increasing knock detection sensitivity by combining knock sensor signal with a control oriented combustion model. Mechanical Systems and Signal Processing. 168:1-11. https://doi.org/10.1016/j.ymssp.2021.108665

Increasing knock detection sensitivity by combining knock sensor signal with a control oriented combustion model

Benjamín Pla[a], Pau Bares[a], Irina Jimenez[a], Carlos Guardiola[b]

[a] *CMT-Motores Termicos, Universitat Politècnica de València, Camino de Vera s/n, E-46022 Valencia, Spain.*
[b] *Universitat Politècnica de València, Departamento de Máquinas y Motores Térmicos Camino de Vera, s/n. 46022 Valencia, Spain.*

Abstract

Knock phenomenon reduces the thermal efficiency and restricts performance improvement in spark-ignited engines. Reliable and rapid knock recognition is crucial for the engine knock control. Amongst the wide set of knock detection techniques, those based on in-cylinder pressure sensors provide the most precise recognition; however, pressure sensors are still affected by challenges such as durability and cost. For on-board applications, knock is usually detected by vibration signal, but the accuracy is limited due to natural vibration and external noises.

In this paper, a knock recognition method based on knock sensor signal is proposed. The method consists of the comparison of a resonance index obtained through the knock sensor signal and a combustion model capable of estimating the fraction of mass burned, and thus being able to estimate if the amplitude in the knock sensor signal is produced by the auto-ignition of certain amount of fuel. The proposed method was compared with a fixed threshold for knock sensor resonance intensity, the improvements were quantified by using as reference a high sensitive knock recognition method based on cylinder pressure. Results show that the proposed method is able to improve the accuracy in over a 10 % of knock detection than using one set threshold over the entire cycle.

Keywords: knock, knock sensor, resonance, combustion model

1. Introduction

Knock is an abnormal combustion in spark ignited (SI) engines which is caused by the auto-ignition of the end gas [1]. The sudden auto-ignition of the end gas depends on local pressure and temperature in the combustion chamber, and excited in-cylinder pressure resonance modes [2]. Knock produces vibration noise, reduces the engine efficiency, and can damage the engine [3].

Knock recognition methods can be divided in two broad groups: direct and indirect methods. Methods in the first group are based on the direct measurement and analysis of in-cylinder pressure [4]. Indirect methods are mainly based on the vibration measurement analysis. Knock recognition techniques based on direct measurement of in-cylinder pressure can be more precise, since the combustion process, and therefore the pressure measurement, is directly influenced by knock phenomenon [5]. Several methods able to detect knocking cycles, even with low intensity, have been published in recent years [6, 2, 7], these methods are highly accurate but their on-board application is limited since in-cylinder pressure sensors have low durability and high cost [8]. On the other hand, recognition techniques based on vibration measurement are widely used in commercial applications since their easy implementation and sensor reliability and cost characteristics.

Due to the mechanical complexity, dynamics and indirect measurement, it is difficult for knock detection methods based on vibration to reach high sensitivity, being able to detect knocking cycles with low intensity. Many authors developed different algorithms in order to process vibration signal and develop knock indexes, such as short Fourier transform [9], wavelet methods [10, 11], empirical mode decomposition [12, 13], variation mode decomposition [14], among others. Other authors develop models, as can be found in [8], where the engine block vibration is represented by a black box model, and knocking cycles are recognized by analyzing the error between the model and the measured signal.

Most of these knock recognition techniques based on knock sensor signal are 0-Dimensional, i.e. only one value is obtained per cycle which represents the oscillation amplitude, which is later compared with a pre-selected threshold in order to distinguish normal combustion from auto-ignition.

In order to develop a more precise knock recognition procedure based on vibration signal, an adaptation to the method developed in [6] is performed by using a combus-

tion model presented in [15, 16]. In any cycle, the combustion model estimates the mass fraction burned (MFB) in crank angle basis. Then, keeping the crank angle basis, the amplitude in the knock sensor signal generated by the auto-ignition of the end gas is determined from the MFB modeled. The obtained amplitude depending on the crank angle is taken as threshold for knock and therefore is after compared with the resonance intensity evolution computed from knock sensor signal to determine the nature of such oscillation.

This work is organized as follows: First section introduces a frequency analysis of knock sensor signal, where a comparison between vibration signal and in-cylinder pressure sensor is performed. Then, the knock recognition procedure is presented, and the minimum oscillation from both signals, knock and in-cylinder pressure, are compared. After, the experimental set-up, and tests performed for illustration and validation proposes are shown. Following the results are discussed, were the proposed method is compared with a fixed threshold over knock sensor resonance intensity during the cycle. Improvements of the present method are quantified by comparing both knock sensor based methods with a high sensitivity in-cylinder pressure based recognition method. Finally, the main conclusions of the work are discussed.

2. Experimental set-up and tests

Experimental tests for illustration and validation proposes were carried out in a turbocharged four stroke light duty SI engine. Main specifications of the engine are collected in Table 1.

Table 1: Engine main specifications

Displaced volume	1300 cc
Stroke	81.2 mm
Bore	72 mm
Compression ratio	10.6:1
Number of cylinders	4
Fuel injection system	GDI

The engine was equipped with a knock sensor (Bosh KS4-R2), in-cylinder, intake manifold and exhaust manifold pressure sensors were installed. The knock sensor was located between cylinders 2 and 3 as is shown in Figure 1. These sensor were acquired as a synchronized task with the crank angle by using a research enconder, with a sampling resolution of 0.2 CAD. In this way, each sample is located in the piston stroke, and thus the volume of the combustion chamber can be phased with these signals if the location of the top dead center is known. When analyzing these signals in the frequency domain, e.g. the short Fourier transform (STFT), constant frequency harmonics are calculate, and a constant time between samples is preferred. For this reason, some authors used crank angle based acquisition and assumed a constant speed during a given cycle. But if during the cycle the engine speed variate, this generates an slight effect in the STFT.

During the experiments, the engine was tested at four steady operating conditions by keeping the speed and intake pressure constant while the spark advance was modified:

- Point 1: 2000 rpm 1.1 bar of intake pressure.
- Point 2: 3000 rpm 1.1 bar of intake pressure.
- Point 3: 3000 rpm 0.8 bar of intake pressure.
- Point 4: 2000 rpm 0.9 bar of intake pressure.

During each operating condition a total of 3000 cycles were recorded by maintaining lambda in stochiometric conditions. The SA was modified in 3 CAD positions.

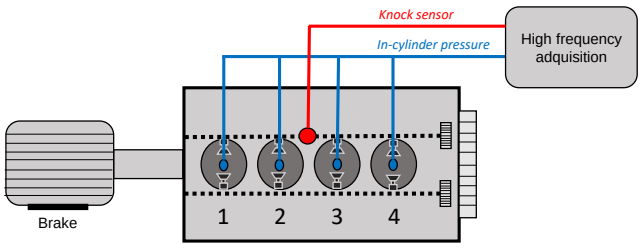

Figure 1: Sensors configuration.

3. Frequency analysis of knock sensor signal

In order to study the non-stationary signal from knock sensor, the Short time Fourier transform (STFT) is used. The STFT allows to analyzed the signal in time-frequency domain by dividing the entire signal into smaller sections, where these portions are assumed to be stationary. In order to divide the signal, a Blackmann-Harris window function is applied, to determine the spectral components of a given portion of the signal [17]. On the top plots the bandpass filtered signal is represented for in-cylinder pressure (left) and knock sensor (right). On the bottom plots of Figure 2, two spectograms are represented: left case the signal is in-cylinder pressure and right case knock sensor. Both spectrograms are obtained by computing the STFT over the signals, with a window length of 20 CAD.

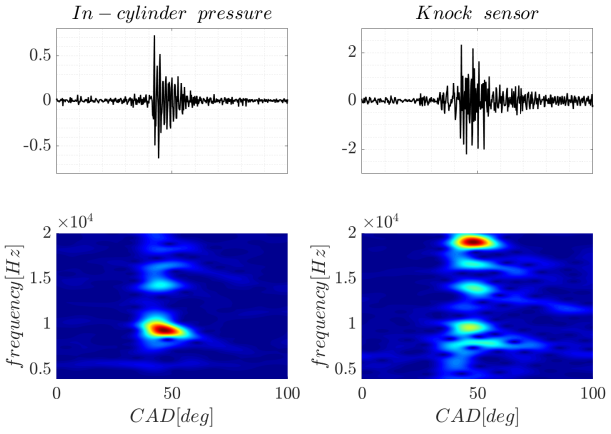

Figure 2: Time-frequency analysis of in-cylinder pressure (left) and knock sensor (right) signals: Band-pass signal (top plots) and spectrograms (bottom plots).

In order to evaluate the correlation between the information contained in knock sensor signal with the in-cylinder pressure signal, an analysis in frequency domain was done. Figure 3 shows the ratio between the cross power spectral density of the in-cylinder pressure and knock sensor signals $P_{p,k}(f)$, to the product of the power spectral density of each signal $P_{p,p}(f)$ and $P_{k,k}(f)$. This functions is known as coherence function and is computed as [18]:

$$C_{p,k}(f) = \frac{|P_{p,k}(f)|^2}{P_{p,p}(f)P_{k,k}(f)} \tag{1}$$

where f represents the different frequencies. Where the power spectral density of a signal x is defined as:

$$P_{x,x}(f) = \sum_{k=-\infty}^{k=\infty} r_{xx}[k]e^{-i2\pi fk} \tag{2}$$

where r_{xx} is the auto correlation function, which is computed as:

$$r_{xx}[k] = \varepsilon\{x^*[n]x[n+k]\} \tag{3}$$

And the cross power spectral density between two signals x and y is defined as following:

$$P_{p,k}(f) = \sum_{k=-\infty}^{k=\infty} r_{xy}[k]e^{-i2\pi fk} \tag{4}$$

where r_{xy} is the cross correlation function, which is computed as:

$$r_{xy}[k] = \varepsilon\{x^*[n]y[n+k]\} \tag{5}$$

The coherence function between the in-cylinder pressure and knock sensor signals ($C_{p,k}$) was evaluated at an steady operating condition in Figure 3, where the grey line represents the evolution of the cross power spectral density in 200 cycles, and the black line is the average of those same cycles.

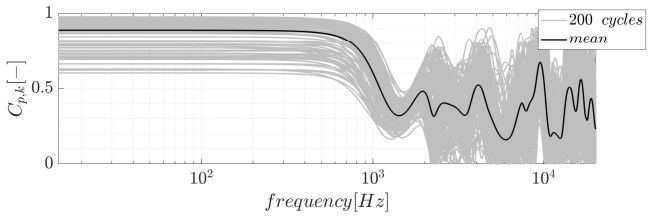

Figure 3: Coherence function between in-cylinder pressure and knock sensor signals over 200 cycles (cylinder 2 operating point 1).

As it can be seen in Figure 3, the highest coherence (above 0.5) is located in the 0-1400 Hz, hence indicating a strong relationship between the spectral components of both signals in that frequency band. Also, frequency peaks can be identified: one at 9 kHz, a second one at 16 kHz and a third at 18 kHz, which corresponds to the first, second and third circumferential resonant modes [19]. Accordingly, low frequency band of the signal is associated with the piston movement, medium frequencies to the combustion process and high frequencies to resonance.

Because of the high coherence at low frequencies, a combustion state estimation can be computed from knock sensor signal. And through high frequencies, an evaluation of resonance in the combustion chamber can be performed.

In this work, the MFB is modeled by using the adaptive combustion model presented in [16], where the pressure peak location is estimated from knock sensor signal by implementing the method described in [**?**], and using this estimation as an observer to update the combustion model.

In order to analyzed the in-cylinder pressure and knock sensor signals at high frequencies the alternative to the Fourier transform presented in [20] is used. This alternative resonance index is computed by windowing the pressure signal such as:

$$I_p(\theta) = \sum_{\theta=\theta_1}^{\theta=\theta_2} w(\theta-\theta_1)p_{bp}(\theta)e^{-2\pi\sum_{\psi=0}^{\psi=\theta}\frac{B\sqrt{\gamma(\psi)p_{lp}(\psi)V(\psi)}}{\pi D\sqrt{m}}}T_s(\theta) \tag{6}$$

where θ_1 and θ_2 define the interval where the resonance analysis is performed, w is a window function of $\theta_2 - \theta_1$ length, p_{bp} the band-pass filtered pressure, and $T_s(\theta)$ is the

sampling period, which is constant only in time-based acquisition or if the instantaneous engine speed fluctuations are negligible, B is the Bessel constant, D is the bore of the cylinder, V the chamber volume, m the trapped mass, and p_{lp} the low-pass in-cylinder pressure.

Analog to the Equation (6), a resonance index can be defined from the knock sensor signal, as following:

$$I_k(\theta) = \sum_{\theta=\theta_1}^{\theta=\theta_2} w(\theta-\theta_1) kn_{bp}(\theta) e^{-2\pi \sum_{\psi=0}^{\psi=\theta} \frac{B\sqrt{\gamma(\psi) kn_{lp}(\psi) V(\psi)}}{\pi D \sqrt{m}} T_s(\theta)} \tag{7}$$

where kn_{bp} and kn_{lp} are the band and low pass knock sensor signal respectively.

The resonance indicator evolution during a knocking cycle computed from knock sensor signal is represented in Figure 4, where it is compared with the resonance indicator obtained from in-cylinder pressure.

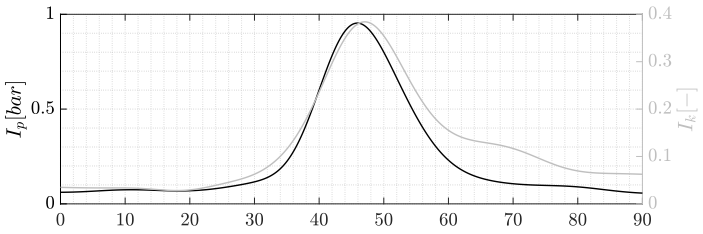

Figure 4: Resonance index from in-cylinder pressure (black) and knock sensor (grey) signal of knocking cycle of case in Figure 2 (cylinder 2 operating point 1).

In order to compare the resonance index from both signals an SA sweep at steady state condition is analyzed, 3000 consecutive cycles are analyzed in Figure 5. On the top plot, the maximum of the resonance index from both signals is shown, while the bottom plot shows the comparison between intensity of the maximum of the resonance index for knock sensor and the difference between the crank angles where the maximum is located for both signals. The color scale represents the maximum resonance intensity obtained from the knock sensor.

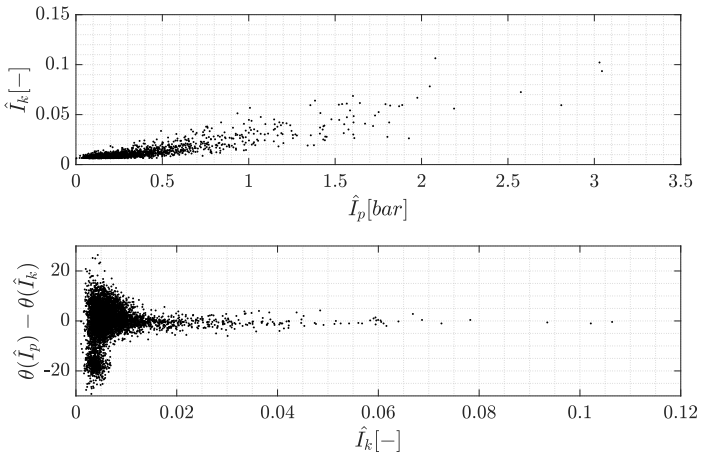

Figure 5: Comparison between resonance index computed by in-cylinder pressure and knock sensor. Maximum of resonance index from in-cylinder pressure against resonance index obtained from knock sensor (top plot). Difference between the maximum location obtained from in-cylinder pressure and knock sensor against maximum amplitude of the index computed from knock sensor (bottom plot). (Cylinder 2 operating point 1)

As expected, Figure 5 shows how the correlation between the crank angles where both signals reach the maximum amplitude increases with resonance intensity. Moreover, the maximum resonance intensity from knock sensor is less correlated with the maximum of pressure sensor due to transmission losses and sensor sensitivity.

In Figure 6 an analysis of the effect of the SA sweeps on the maximum resonance index in terms of localization an amplitude for both sensors is performed. In particular, Figure 6 shows, for different SA settings, the number of occurrences of the maximum resonance index in terms of localization (x axes) and amplitude (y axes) is shown. Top plots corresponds to results from in-cylinder pressure sensor, and bottom plots show the results from knock sensor.

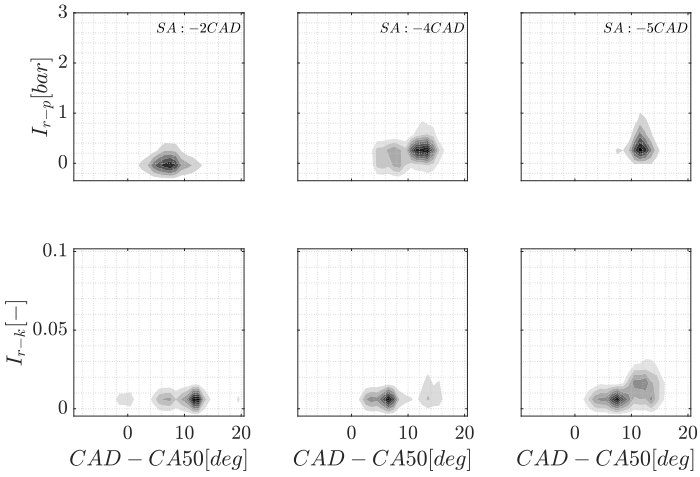

Figure 6: Amplitude versus location histograms of the resonance index obtained from in-cylinder pressure (top) and knock sensor (bottom) signals.

As is shown in Figure 6, in low probability knocking cycles, i.e SA = - 2 CAD, the maximum of the resonance index from in-cylinder pressure I_{r-p} is located between -5 and 5 CAD of the CA50. For the knock sensor case, I_k, and additional cloud of low intensity at 20 CAD after CA50 appears, this is associated with noise of the signal. When advancing the SA (SA = -4 and -5 CAD) a cloud located around 0 and 10 CAD after CA50 varying its intensity emerge for both cases. This new could of points represents the knocking events, which are located near the EOC, and the intensity levels vary between low to high amplitudes. For this analysis amplitudes located after CA100 and before CA10 are not considerate.

Because the distribution of the maximums is similar for both sensors, a method based on [6] can be developed to identify knocking cycles from vibration measurement.

4. Model based knock recognition method

In this section a method which combines a combustion model and the knock recognition method presented in [6] is explained. From the combustion model presented in [**?**], it is possible to model the MFB cycle-to-cycle variability from ECU variables. From the modeled MFB and analog to the method found in [6], the minimum oscillation required derived from the first law of thermodynamics can be estimated as:

$$I_{k,min} = G_k \frac{\kappa - 1}{V} m_f H_p (1 - MFB_{model}) \qquad (8)$$

where G_k is a constant to be calibrated and MFB_{model} the MFB as estimated by the combustion model.

$I_{k,min}$ computed from Eq (8) is used to determine the expected intensity if the end-gas auto ignite, i.e if the end gas auto ignite at the begining of the combustion a great resonance amplitude is expected, because almost all the fuel will be auto ignited. On the other hand, at the end of the combustion, the resonance intensity is expected to be much lower.

The scheme of the knock recognition procedure proposed is shown in Figure 7.

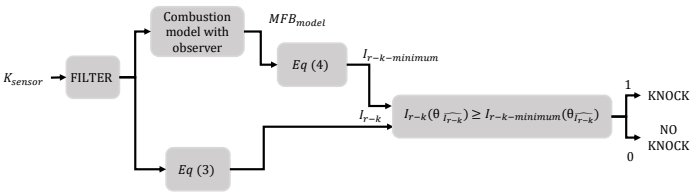

Figure 7: Knock recognition procedure based on knock sensor frequency analysis and combustion model.

From knock sensor signal, feedback information from all four cylinders can be extracted as is shown in Figure 8, where on top plot the in-cylinder pressure signal of a given cycle is represented, and on the bottom plot the knock sensor signal with the sample window for each cylinder is represented. The window considerate for each cylinder was from the intake valve closing angle position up to the exhaust valve opening.

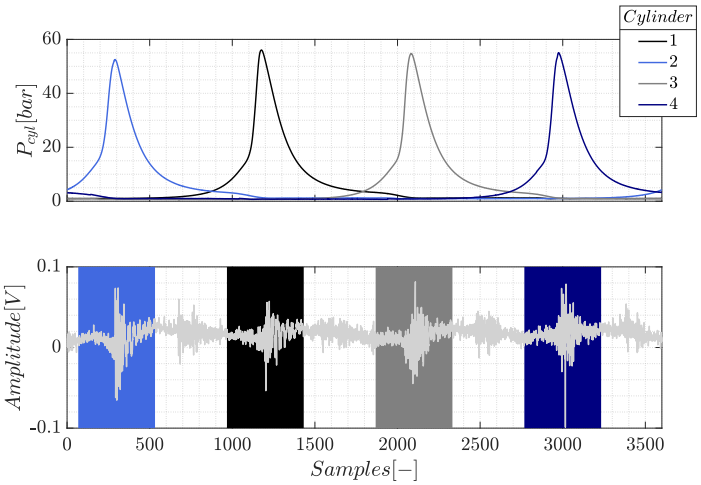

Figure 8: Cylinder information from knock sensor signal: No triggered in-cylinder pressure signals (top plot) and knock sensor signal with cylinders sample window (bottom plot).

The minimum oscillation required to the end gas to auto ignited is represented in Figure 8 (top plot) by computing the MFB from in-cylinder pressure signal (black

line) and from the combustion model (grey line). On the bottom plot the relative error between the I_{min} computed by the MFB obtained from in-cylinder pressure and the combustion model is represented over 200 cycles.

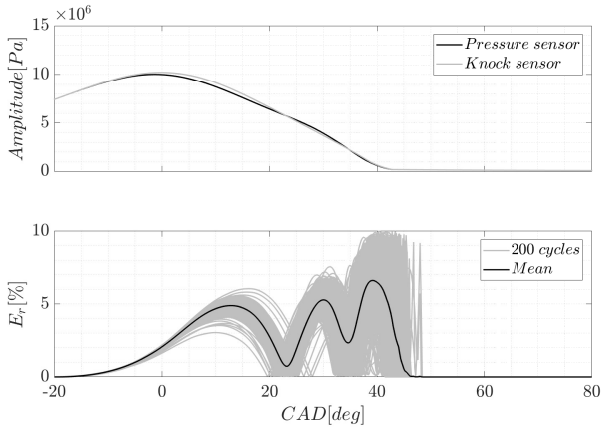

Figure 9: Minimum expected intensity to the end gas to auto ignited for two cases: MFB computed by the in-cylinder pressure (black) and by combustion model (grey).

As it can be seen in Figure 9 (top plot), by combining the knock sensor signal and the combustion model is possible to represent the amplitude that a certain amount of end-gas would generate if it auto-ignite, being the relative error between computing the MFB from in-cylinder pressure and combustion model bellow 10 %.

According to Figure 5, the maximum of the resonance index location from knock sensor signal is representative of the index computed from in-cylinder pressure when the amplitude of the oscillation is high. In order to quantify such amplitude the absolute error between the maximum resonance index location from both signals, computed as the difference $E_a = \theta(\hat{I}_k) - \theta(\hat{I}_p)$, is represented in Figure 10 as a function of the amplitude from knock sensor signal $\hat{I}_k$. A tolerance of ±4 CAD is represented in dashed line, and in continuous line the sensitivity of knock sensor, i.e below this amplitude the cycle is classified as no knocking.

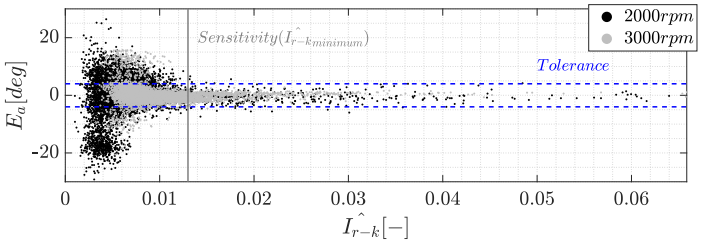

Figure 10: Resonance sensitivity for knock sensor signal for two operating condition cases over cylinder 2 (Operating point 1 and 2).

5. Results and discussion

In this section, the proposed methodology based on knock sensor signal is compared with two knock recognition methodologies based in pressure sensor: classical MAPO definition and a the low knocking cycle method presented in [6], and a fixed threshold based on the resonance amplitude from knock sensor signal.

In Figure 11, MAPO value obtained from in-cylinder pressure is compared with the amplitude $\hat{I_{r-k}}$ obtained from knock sensor signal over operating conditions 1 and 2. The fitted line is represented in dashed grey line and the MAPO threshold considerate for this analysis in dashed blue line. The intersection between the two lines (I_{k-th}) is used as a fixed threshold to classify knocking cycles from knock sensor signal.

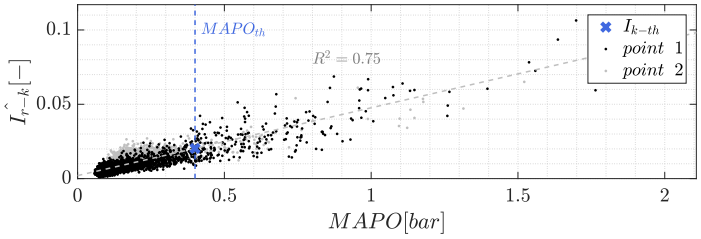

Figure 11: Maximum resonance index against MAPO amplitude over operating condition 1 and 2 (cylinder 2).

In Figure 12, the MAPO amplitude is represented against the maximum resonance index from the knock sensor, $\hat{I_{r-k}}$, over a SA sweep during operating point 1. 5000 cycles are represented in grey dots, knocking cycles as classified by the proposed procedure based on knock sensor are represented in black crosses, while knocking cycles recognized by method presented in [6] are represented in dark grey. Three amplitudes are highlighted in hatched line: in x axes the MAPO threshold used to differentiate knocking from combustion (0.4 bar), at the right of this limit knocking cycles are detected, and in y axes the sensitivity amplitude from knock sensor signal and the fixed threshold I_{r-th} for knock resonance index.

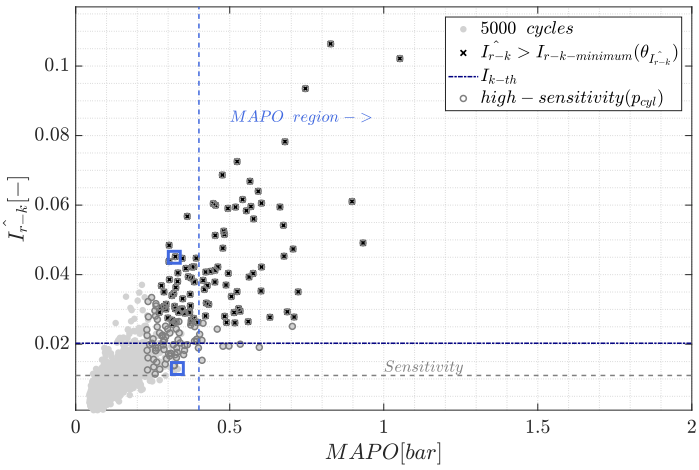

Figure 12: Maximum resonance index against MAPO amplitude over operating condition 1 cylinder 2. Black crosses indicates knocking recognition by proposed method. (Cylinder 2 operating point 1)

As is shown in Figure 12, most of knocking cycles classified with MAPO method are detected by the proposed technique. A few cycles with a MAPO intensity over 0.4 bar are not recognized by the proposed method, this is due to errors in the combustion model caused by noise from other cylinders in knock sensor signal. Moreover, some cycles at the left of the established MAPO limit are recognized as knocking by the proposed method, to clarify this point two cycles (labeled with squares in Figure 12) are shown as an example in the Figure: left plot shows a cycle recognized by knock sensor methodology and right plot a non-recognized cycles.

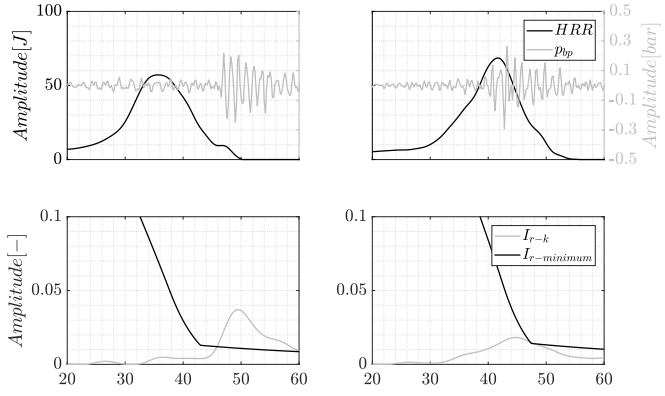

Figure 13: Detail points labeled in Figure 12. Band pass in-cylinder pressure and HRR (Top plots), resonance index evolution computed from knock sensor and minimum oscillation. Left case recognized as knock and right case normal combustion. (Cylinder 2 operating point 1)

Analyzing Figure 13, both cases have a MAPO amplitude of 0.2 bar, on the left case the resonance is excited at the end of the combustion and a second peak over the HRR appears, on the right case the resonance is excited during the combustion. For this reason, it is not possible to decrease MAPO threshold, i.e no-knocking cycles can be confused with normal combustion. But the method proposed in [6] is able to differentiate low-knocking cycles from combustion. For this reason, the high sensitivity knock recognition method presented in [6] will be used to quantify the improvements of the proposed method.

In order to quantify the accuracy of the proposed method two confusion matrix are presented in Figure 14. Left plot shows the low-knock recognition method presented in [6] compared with a fixed threshold for knock sensor, i.e. knock is classified when $I_{r-k} >= I_{r-th}$. Right plot illustrate the comparison between the high sensitivity recognition method based in in-cylinder pressure with the proposed method.

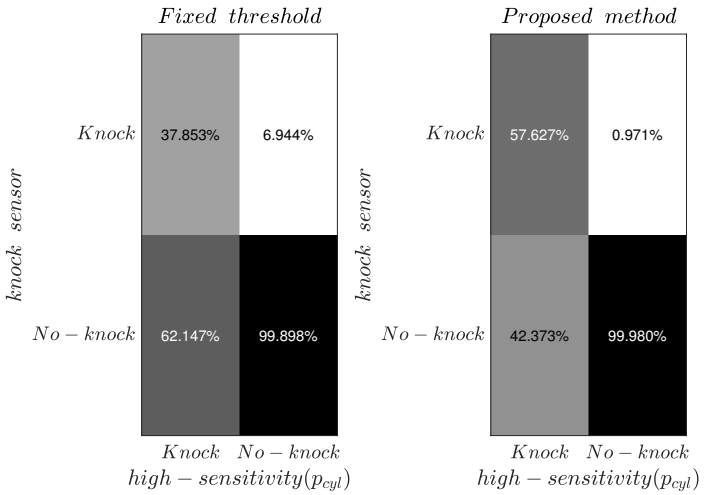

Figure 14: Confusion matrix between knock sensor based recognition and high sensitivity method presented in [6]: left plot fixed threshold and right plot proposed method.

As is shown in Figure 14, at operating condition 1, the proposed method is able to recognize over a 20 % of knocking cycles when comparing with a fixed threshold method, while reducing the false negatives cases.

The method was applied over the four cylinders, in Figure 15 the knock probability for the method proposed is compared with the knock probability for two methods based on in-cylinder pressure and by applying a fixed threshold for knock sensor maximum resonance amplitude. The analysis is performed over different SA setting.

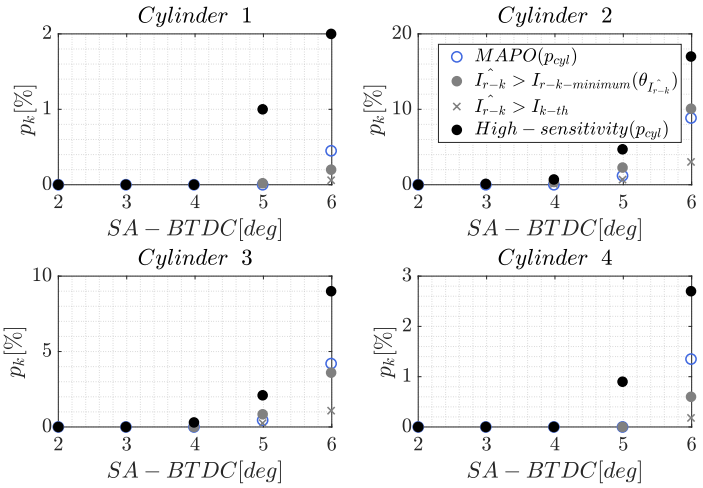

Figure 15: Knock probability as a function of the SA for all cylinders. (cylinder 2 operating point 1).

As is shown in Figure 15, the proposed method based on knock sensor signal is not able to distinguish all low knocking cycles but is able to recognize almost the same knock probability that applying a MAPO threshold of 0.4 bar over the in-cylinder pressure.

The four operating conditions presented in Section 2 are analyzed in Figure 16. For tested operating conditions, the knock probability for the proposed method is compared with the two in-cylinder pressure based methods and with a fixed threshold for knock sensor. The analysis was performed over cylinder 2.

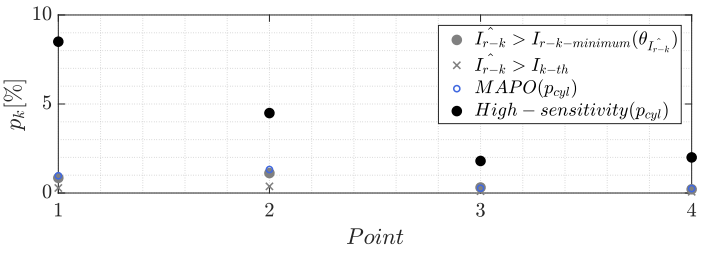

Figure 16: Knock probability for all operating conditions tested presented in section 2.

Once again, method proposed is able to recognize a similar knock probability that when applying a MAPO threshold of 0.4 bar over different operating conditions and cylinders, and improves the estimation than when applying a fixed threshold. This allows to extend the conclusions from operating point 1 to the rest of the engine operating map.

Over all four tested points the improvement is illustrated in Figure 17, where the low-knocking cycle recognition method presented in [6] is compared with the fixed threshold (left plot) and with the proposed method (right plot).

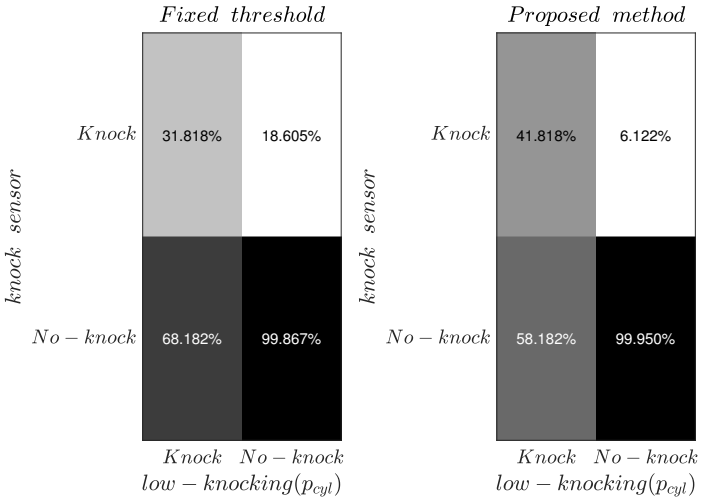

Figure 17: Knock probability for all operating conditions tested presented in section 2.

6. Conclusions

This article presents a knock recognition method based on knock sensor signal. The vibration signal was processed in two different frequencies bands. The information extracted from low frequencies was used to update a combustion model and estimate the mass fraction burned. While high frequencies were used to compute a resonance index. Knock recognition was performed by using an adaptation of the method proposed in [15], which was originally use for the in-cylinder pressure. The method was validated over 2 engine speed and 2 engine loads, i.e. being able to recognize a similar knock probability than when applying a MAPO threshold of 0.4 bar.

As can be seen in the confusion matrix in Figure 17, the method shows an improvement in knocking cycle recognition than applying a fixed threshold for the maximum resonance intensity. The proposed method exhibits an improvement of an 10 % on the accuracy, than the fixed threshold classification. Future work is devote to develop a knock control by applying this recognition method.

7. Acknowledgments

Irina A. Jimenez received a funding through the grant 132GRISOLIAP/2018/132 from the Generalitat Valenciana and the European Social Fund.

References

[1] J. B. Heywood, Internal combustion engine fundamentals, McGraw-Hill Education, 2018.

[2] P. Bares, D. Selmanaj, C. Guardiola, C. Onder, A new knock event definition for knock detection and control optimization, Applied Thermal Engineering 131 (2018) 80–88.

[3] R. Nates, A. Yates, Knock damage mechanisms in spark-ignition engines, SAE transactions (1994) 1970–1980.

[4] X. Zhen, Y. Wang, S. Xu, Y. Zhu, C. Tao, T. Xu, M. Song, The engine knock analysis–an overview, Applied Energy 92 (2012) 628–636.

[5] R. Worret, S. Bernhardt, F. Schwarz, U. Spicher, Application of different cylinder pressure based knock detection methods in spark ignition engines, SAE Transactions (2002) 2244–2257.

[6] B. Pla, J. De La Morena, P. Bares, I. Jiménez, Knock analysis in the crank angle domain for low-knocking cycles detection, Tech. rep., SAE Technical Paper (2020).

[7] R. Novella, B. Pla, P. Bares, I. Jiménez, Acoustic characterization of combustion chambers in reciprocating engines: An application for low knocking cycles recognition, International Journal of Engine Research (2020) 1468087420980565.

[8] D. Siano, M. A. Panza, A nonlinear black-box modeling method for knock detection in spark-ignition engines, in: AIP Conference Proceedings, Vol. 2191, AIP Publishing LLC, 2019, p. 020137.

[9] K. Akimoto, H. Komatsu, A. Kurauchi, Development of pattern recognition knock detection system using short-time fourier transform, IFAC Proceedings Volumes 46 (21) (2013) 366–371.

[10] F. Bi, T. Ma, X. Wang, Development of a novel knock characteristic detection method for gasoline engines based on wavelet-denoising and emd decomposition, Mechanical Systems and Signal Processing 117 (2019) 517–536.

[11] A. Moshrefi, O. Shoaei, Effective method for knock signal denoising in internal combustion engine, International Journal of Automotive Technology 18 (5) (2017) 769–777.

[12] F. Bi, T. Ma, J. Zhang, Knock feature extraction in spark ignition engines using eemd-hilbert transform, Tech. rep., SAE Technical Paper (2016).

[13] A. Moshrefi, N. Alavi, H. Aghababa, Knock detection improvement applying quantum signal processing method in automotive system, in: Proceedings of the 10th Hellenic Conference on Artificial Intelligence, 2018, pp. 1–4.

[14] F. Bi, X. Li, C. Liu, C. Tian, T. Ma, X. Yang, Knock detection based on the optimized variational mode decomposition, Measurement 140 (2019) 1–13.

[15] B. Pla, J. De la Morena, P. Bares, I. Jiménez, Cycle-to-cycle combustion variability modelling in spark ignited engines for control purposes, International Journal of Engine Research 21 (8) (2020) 1398–1411.

[16] B. Pla, J. De La Morena, P. Bares, I. Jiménez, Adaptive in-cylinder pressure model for spark ignition engine control, Fuel 299 (2021) 120870.

[17] S. Vulli, J. Dunne, R. Potenza, D. Richardson, P. King, Time-frequency analysis of single-point engine-block vibration measurements for multiple excitation-event identification, Journal of Sound and Vibration 321 (3-5) (2009) 1129–1143.

[18] O. Chiavola, G. Chiatti, L. Arnone, S. Manelli, Combustion characterization in diesel engine via block vibration analysis, Tech. rep., SAE Technical Paper (2010).

[19] C. S. Draper, The physical effects of detonation in a closed cylindrical chamber (1935).

[20] C. Guardiola, B. Pla, P. Bares, A. Barbier, An analysis of the in-cylinder pressure resonance excitation in internal combustion engines, Applied Energy 228 (2018) 1272–1279.